# A Multimode Fiber Refractive Index Sensor

H. Apriyanto, G. Ravet, O. D. Bernal, M. Cattoen, F. Lizion, H. C. Seat
LAAS-CNRS, Université de Toulouse, CNRS, INP
Toulouse, France
haris.apriyanto@enseeiht.fr

V. Chavagnac
Géosciences Environnement Toulouse UMR5563
OMP, Université de Toulouse, CNRS, IRD
Toulouse, France

***Abstract*— We present a simple refractive index sensor based on multimode fibers realized by stripping three different lengths of cladding. We theoretically explain and experimentally validate three mechanisms occurring in the multimode fiber for sensing surrounding refractive index. This sensor has been demonstrated at 1550 nm for a wide range of refractive index variation from 1.3164 to 1.608. Our sensor is very sensitive for measuring refractive index values lower than but close to the refractive index value of the fiber core.**

***Keywords—Refractive index sensor; Refractometer; Multimode fiber sensor; Evanescent wave; Stripped cladding***

## I. INTRODUCTION

The refractive index (RI) sensor, also commonly known as the refractometer, is widely used in the food, chemical, biomedical industries, as well as in environmental monitoring, etc. Due to their good sensitivity, RI sensors have been used for measuring methane concentration by using cryptophane based traps in polymeric PDMS to absorb the methane molecules leading to refractive index variation from 1.412 to 1.413 with a sensitivity 5.5 RIU/nM at 830 nm of wavelength [1].

The principal techniques employed for measuring RI, an optical phenomenon, consist of prisms [2-3], fiber-based surface plasmon resonance (SPR) [4], microstructured fiber-based SPR [5], Fresnel reflection at an optical fiber interface [6-8], fiber Bragg grating [9-10], fiber ring laser [11], nanometric plasmonic [12], multimode fiber [13-15], and tapered multimode optical fiber [16].

In this paper, we present a simple yet elegant multimode fiber sensor for measuring RI over a relatively wide dynamic range where the sensing area is a section of stripped fiber cladding. The impact of the length of stripped cladding section is also investigated to estimate the sensor's sensitivity over the useful RI range. The advantages of this sensor are its simplicity, cost-effectiveness, wide range and high sensitivity for RI values lower than but near to the RI of the fiber core.

## II. PRINCIPLE OF OPERATION

In wave optics, the propagation of the injected laser beam in the optical fiber can be represented in terms of modes. To define the number of modes (M), the V-parameter can be used and is a function of the relative RI difference between the fiber core ($n_{co}$) and cladding ($n_{cl}$), operational wavelength ($\lambda$), and core radius (a), governed by the relationship [17]

$$M = \frac{4}{\pi^2} V^2 \quad (1)$$

where $V$ is given by $V = \frac{2\pi a}{\lambda}\sqrt{{n_{co}}^2 - {n_{cl}}^2}$ .

In a step-index fiber, each mode that propagates in the optical fiber has a unique propagation constant which is proportional to the effective guide index ($n_{eff}$) and wavenumber (k) [18] given by

$$\beta = k n_{eff} \quad (2)$$

However, through ray optics analysis, this mode can also be represented as a ray propagating in the core region at a certain angle ($\theta_a$), as shown in Fig. 1, with

$$n_{eff} = n_{co} sin\theta \quad (3)$$

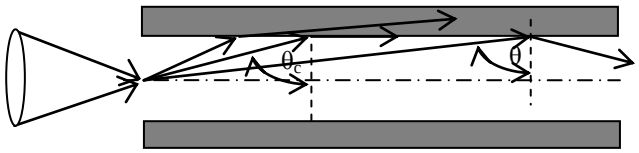


Fig. 1. Principle of propagation in step-index fiber.

where the possible angles within which the ray can propagate in the core should respect $\theta_c \leq \theta \leq 90°$. The guided modes are thus within $n_{co} sin\,\theta_c \leq n_{co} sin\,\theta \leq n_{co} sin\,90$, corresponding to possible effective indices of $n_{cl} \leq n_{eff} \leq n_{co}$. The number of guided modes, and hence the transmitted optical power, in the fiber are thus highly dependent on RI variation of the outer cladding layer, potentially rendering the MMF a highly sensitive refractometer. For RI measurements, a section of the MMF outer cladding layer is removed and the exposed fiber core serving as the sensing region is arranged to be in contact with the external medium subject to RI variation.

The length of the stripped cladding section is here investigated as a function of the MMF sensitivity to RI variations and is correlated to 3 possible operating conditions occurring in the sensing region with respect to the RI of the external sensing medium ($n_{ms}$), namely: a) $n_{ms} \leq n_{cl}$, b) $n_{cl} \leq n_{ms} \leq n_{co}$, and c) $n_{co} \leq n_{ms}$.

For $n_{ms} \leq n_{cl}$ (or Zone I), the RI of the medium is detected via the phenomenon of evanescent wave absorption that exists during propagation when the modes are guided by total internal reflection (TIR). The evanescent field is generated at the core-cladding interface, and penetrates into the cladding (Fig. 2) to a certain depth ($d_p$) [19] given by

$$d_p = \frac{\lambda_0}{2\pi\sqrt{sin^2\theta - \left(\frac{n_{cl}}{n_{co}}\right)^2}} \quad (4)$$

Further, the evanescent wave is attenuated in the cladding. The cladding attenuation coefficient $\gamma$ is proportional to the total attenuation coefficient α and to the fraction of the guided power $r$, $\gamma = r\alpha$, with $r = \frac{P_{cladd}}{P_{total}}$. Since we removed the cladding and replaced it by a medium for sensing, the power transmitted at the sensing length ($L$) is given by

$$P(L) = P(0)\exp(-\gamma L) \quad (5)$$

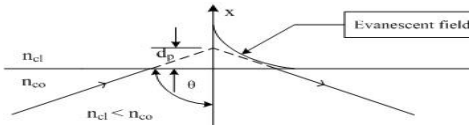


Fig. 2. Evanescent wave in the cladding region (Zone I).

For the second condition, illustrated in Fig. 3, where $n_{cl} \leq n_{ms} \leq n_{co}$ (Zone II), the RI variation is due to 2 phenomena: a) modification to the critical angle since $\theta_c = arc\sin(n_{cl}/n_{co})$, leading to the variation of the number of guided modes, and b) the evanescent wave absorption by the external medium since TIR still occurs under these conditions. Hence, there should be a stronger variation of the transmitted power than Zone I over the same variation in RI.

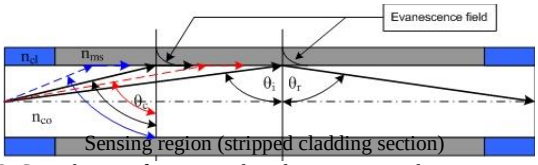


Fig. 3. Contributions from critical angle variation, and evanescent wave absorption for $n_{cl} \leq n_{ms} \leq n_{co}$ (Zone II).

Finally, when $n_{co} \leq n_{ms}$ (Zone III), the laser beam in the MMF core is propagated by external reflection. This phenomenon occurs since the core index is lower than that of the cladding at an incident angle close to 90°. This implies that the external reflection only occurs for lower order modes. In this condition, no evanescent wave interacts with the sensing medium as illustrated in Fig. 4.


Fig. 4. External reflection in MMF (Zone III).

Since the sensing medium has higher RI than the core, a portion of the ray at the boundary will be transmitted to the exterior while the rest will be reflected back into the core. Using Snell's law, the reflected angle ($\theta_r$) which is equal to the incident angle ($\theta_t$), and the transmitted angle ($\theta_t$) are related by

$$\frac{sin\ \theta_t}{sin\ \theta_i} = \frac{n_{co}}{n_{ms}} \quad (5)$$

while the reflection coefficients for the P- and S-polarizations are given by Fresnel relations [20]:

$$r_p = \frac{tan\ (\theta_i - \theta_t)}{tan\ (\theta_i + \theta_t)},\ r_s = \frac{sin\ (\theta_i - \theta_t)}{sin\ (\theta_i + \theta_t)} \quad (6)$$

The resulting total reflectivity R is thus given by

$$R = \frac{1}{2}(r_p{}^2 + r_s{}^2) \quad (7)$$

## III. Experiment Setup

The sensing fiber employed is a multimode plastic-clad-silica (PCS) fiber with a numerical aperture (NA) of 0.48, and core and cladding diameters of 200 µm and 230 µm, respectively. The cladding layer is removed to obtain three different sensing lengths of 1 cm, 2.5 cm and 4 cm. Further, in order to excite all possible modes in this MMF, a microscope objective (MO) with an NA of 0.65 is employed.

To detect the RI of the medium, the variation of the optical power transmitted in the fiber is measured. In addition, to compensate ambient temperature perturbations, a differential set-up is exploited, with one MMF serving as the reference fiber ($P_{ref}$) and the second as the sensing fiber ($P_{sens}$), as shown in Fig. 5.

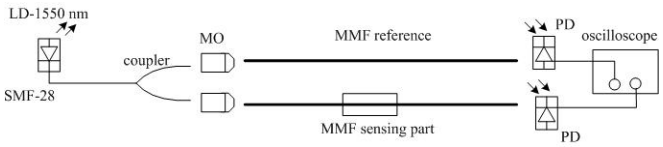


Fig. 5. Schematic diagram of the experimental set-up.

The RI variation of the medium is obtained from a combination of glycerol and water for RI from 1.3164 to 1.4569 (at a wavelength of 1550 nm)[21], and calibrated oils for RI beyond 1.4569.

## IV. Results and Discussion

The RI measurements are carried out by normalizing the power transmitted by the sensing MMF with respect to the reference MMF over the RI range 1.3164 - 1.608. From the available NA and fiber core data ($n_{co}$ ~1.44402), the fiber cladding index, $n_{cl}$, is estimated to be 1.362.

The experimental results are plotted in Figs. 6 and 7 for three different lengths of sensing region. To facilitate the analysis of the results, both curves are divided into the three conditions (or zones) as previously explained, i.e. a) $n_{ms} \leq 1.362$, b) $1.362 \leq n_{ms} \leq 1.44402$, and c) $n_{ms} \geq 1.44402$. Subsequently, to estimate the sensitivities of this sensor, we derived the function of the curves in Fig. 6 for each of the sensing lengths, the results of which are plotted in Fig. 7.

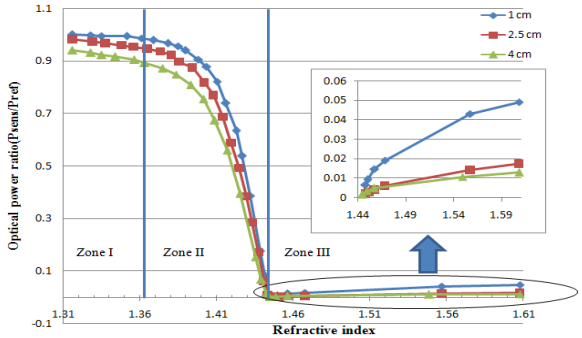


Fig. 6. Optical power ratio ($P_{sens}$/ $P_{ref}$) versus RI variation.

According to Fig. 7, for Zone I, a better sensitivity is achieved by the 4 cm stripped cladding, compared with the 1 cm and 2.5 cm stripped claddings. This confirms the

exponentially decreasing transmitted power due to evanescent wave absorption as a function of the stripped cladding length described by (5). The highest sensitivity is achieved at the end of Zone II with a -32.93 $RIU^{-1}$, -28 $RIU^{-1}$ and -22.98 $RIU^{-1}$ for the 1 cm, 2.5 cm and 4 cm stripped cladding, respectively. This sharp decrease is due to the larger losses of the lower order modes. However, at the beginning of Zone II (1.365-1.417), which can be applied for methane sensing, the longer cladding section (4 cm) has a better sensitivity than the others. For Zone III, since external reflection occurs in the sensing region, most of the optical power is transmitted to the exterior of fiber, thus significantly reducing the guided power in the core. According to (6) and (7), the guided optical power increases for increasing RI.

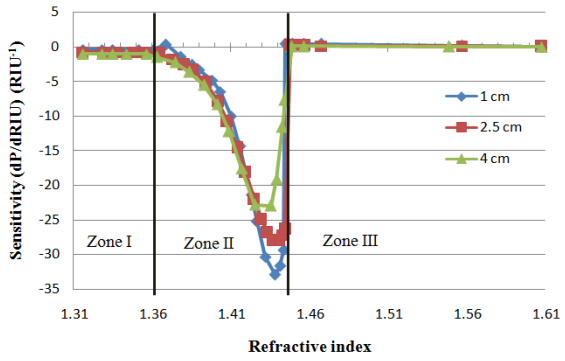


Fig. 7. Sensitivity of the sensor versus RI variation ($P=P_{sens}/P_{ref}$).

Due to a lower number of reflections (N) at the core-medium boundary, the guided power is thus higher for the shorter stripped length. By adapting (7), the guided power can be calculated by $P(N) = P_0(R)^N$, with $P_0$ the incident power. For a fiber with a core diameter $a$ and a sensing length L, $N \approx L/(a \tan \theta_i)$. Since the value of R in (7) is always less than 1, more reflections lead to a reduced guided power. Figs. 6 and 7 show that in the case of external reflection, the shorter stripped clad fiber has a better sensitivity.

## V. Conclusion

A refractive index sensor based on the multimode fiber was conceived to measure refractive indices from 1.3164 to 1.608 at a wavelength of 1550 nm. We described three sensitivity zones with respect to the RI of the cladding and the core of the fiber. In the first zone, a stripped clad fiber of 4 cm has a better sensitivity than both the 1 cm and 2.5 cm devices. The sensitivity is highest at the end of the second zone, and is better for the 1 cm stripped cladding. Finally, for the third zone, less power is guided but increases for increasing refractive index, with a better sensitivity obtained for a shorter length of the stripped clad.

## Acknowledgment

Haris Apriyanto acknowledges the Indonesia Endowment Fund for Education (LPDP) for a PhD scholarship.

## References

[1] C. Boulart, M. C. Mowlem, D. P. Connelly, J.-P. Dutasta, and C. R. German, "A novel, low-cost, high performance dissolved methane sensor for aqueous environments.," Opt. Express, vol. 16, no. 17, pp. 12607–12617, 2008.

[2] M. Astrua and M. Pisani, "Prism refractive index measurement at INRiM," Meas. Sci. Technol., vol. 20, no. 9, p. 095305, 2009.

[3] J. Zhou, Y. Wang, C. Liao, B. Sun, J. He, G. Yin, S. Liu, Z. Li, G. Wang, X. Zhong, and J. Zhao, "Intensity modulated refractive index sensor based on optical fiber Michelson interferometer," Sensors Actuators B: Chem., vol. 208, pp. 315–319, 2015.

[4] A. K. Pathak, V. Bhardwaj, R. K. Gangwar and V. K. Singh, "SPR Based Fiber Sensor to Measure Refractive Index of Glycerol and Acetone," ICMAP, pp. 2–4, Dhanbad (India), 11-13 Dec 2015.

[5] D. F. Santos, A. Guerreiro, and J. M. Baptista, "SPR microstructured D-type optical fiber sensor configuration for refractive index measurement," IEEE Sensors J., vol. 15, no. 10, pp. 5472–5477, 2015.

[6] W. Xu, X. G. Huang, and J. S. Pan, "Simple fiber-optic refractive index sensor based on fresnel reflection and optical switch," IEEE Sensors J., vol. 13, no. 5, pp. 1571–1574, 2013.

[7] J. R. Zhao, X. G. Huang, W. X. He, and J. H. Chen, "High-resolution and temperature-insensitive fiber optic refractive index sensor based on fresnel reflection modulated by Fabry-Perot interference," J. Lightwave Technol., vol. 28, no. 19, pp. 2799–2803, 2010.

[8] C. L. Zhao, J. Li, S. Zhang, Z. Zhang, and S. Jin, "Simple fresnel reflection-based optical fiber sensor for multipoint refractive index measurement using an AWG," IEEE Photon. Technol. Lett., vol. 25, no. 6, pp. 606–608, 2013.

[9] A. Iadicicco, A. Cusano, S. Campopiano, A. Cutolo, and M. Giordano, "Thinned fiber Bragg gratings as refractive index sensors," IEEE Sensors J., vol. 5, no. 6, pp. 1288–1294, 2005.

[10] A. Iadicicco, A. Cusano, A. Cutolo, R. Bernini and M. Giordano, "Thinned fiber Bragg gratings as high sensitivity refractive index sensor," IEEE Photon. Technol. Lett., vol. 16, no. 4, pp. 1149–1151, 2004.

[11] X. Zhang, Z. Liu, L. Xie, and W. Peng, "Refractive index sensor based on fiber ring laser," IEEE Photon. Technol. Lett., vol. 28, no. 4, pp. 524–527, 2016.

[12] X. P. Jin, X. G. Huang, J. Tao, X. S. Lin, and Q. Zhang, "A novel nanometeric plasmonic refractive index sensor," IEEE Trans. Nanotechnol., vol. 9, no. 2, pp. 134–137, 2010.

[13] H. Fukano, T. Aiga, and S. Taue, "High-sensitivity fiber-optic refractive index sensor based on multimode interference using small-core single-mode fiber for biosensing," Jpn. J. Appl. Phys., vol. 53, no. 4, Spec. Issue, pp. 6–10, 2014.

[14] C.-H. Chen, Y.-C. Chen, J.-N. Wang, L.-K. Chau, J.-L. Tang, and W.-T. Wu, "Multimode fiber Mach-Zehnder interferometer for measurement of refractive index," Proc. IEEE Sensors 2010, vol. 2, pp. 61–64, 2010.

[15] M. Fiber, "High refractive index liquid level measurement via coreless multimode fiber," IEEE Photon. Technol. Lett., vol. 27, no. 20, pp. 2111–2114, 2015.

[16] J. H. Kim, B. C. Kim, Y. T. Byun, Y. M. Jhon, S. Lee, D. H. Woo, and S. H. Kim, "High resolution refractive index sensing with cladded multimode tapered optical fibre," Jpn. J. Appl. Phys., Part 1 Regul. Pap. Short Notes Rev. Pap., vol. 43, no. 2, pp. 608–610, 2004.

[17] B. E. A. Saleh, M. C. Teich, Fundamental of Photonics, New Jersey: John and Wiley & Sons, Inc, 2007.

[18] M. S. Wartak, Computational Photonics: An Introduction with MATLAB, New York: Cambridge University Press, 2013.

[19] S. John, "Evanescent Wave Fibre Optic Sensors : Design, Fabrication and Characterization," PhD Thesis, India: Cochin University of Science & Technology, 2000.

[20] P. Taylor, A. I. Lvovsky, and A. I. Lvovsky, "Fresnel Equations," in Encycl. Opt. Eng., Oxford: Taylor & Francis, 2013, pp. 37–41.

[21] J. E. Saunders, C. Sanders, H. Chen, and H. P. Loock, "The refractive index of common solvents and solutions at 1550 nm," Applied Optics, vol. 55, no. 4, pp. 947-953, 2016